The Journal of Experimental Biology 201, 2159–2170 (1998)
Printed in Great Britain © The Company of Biologists Limited 1998
JEB1471

BURROW VENTILATION IN THE TUBE-DWELLING SHRIMP *CALLIANASSA SUBTERRANEA* (DECAPODA: THALASSINIDEA)

II. THE FLOW IN THE VICINITY OF THE SHRIMP AND THE ENERGETIC ADVANTAGES OF A LAMINAR NON-PULSATING VENTILATION CURRENT

EIZE J. STAMHUIS* AND JOHN J. VIDELER
Department of Marine Biology, University of Groningen, PO Box 14, 9750 AA Haren, the Netherlands
*e-mail: e.j.stamhuis@biol.rug.nl

Accepted 5 May; published on WWW 25 June 1998

Summary

The ventilation flow in the vicinity of the pleopod-pumping thalassinid shrimp *Callianassa subterranea* in an artificial transparent burrow has been mapped using particle image velocimetry. The flow in the tube in front of the shrimp was unidirectional, laminar and steady, with a parabolic cross-sectional velocity profile. The mean flow velocity was 2.0±0.1 mm s^{-1}. The flow passed the thorax of the shrimp along the lateral and ventral sides. Ventral to the abdomen, the flow was dominated by the metachronally oscillating pleopods. The water around a pleopod is accelerated caudally and ventrally during the power stroke, and decelerated to a much lesser extent during the recovery stroke owing to a reduction in pleopod area. On average, the flow ventral to the abdomen converged towards the small opening underneath the telson, simultaneously increasing in velocity. A jet with a core velocity of 18–20 mm s^{-1} entered the area behind the shrimp from underneath the telson. This caused a separation zone with backflow caudal to the telson. Owing to the high rates of shear, the jet diverged and re-adjusted to a parabolic cross-sectional profile within 1–2 body lengths behind the shrimp, showing no traces of pulsation. The metachronal pleopod movements in combination with the increase in flow velocity at the constriction in the tube caused by the uropods and the telson probably prevented pulsation. The energetic consequences of pulsating and steady flows in combination with several tube configurations were evaluated. The results suggested that, by constricting the tube and keeping the flow steady, *C. subterranea* saves on ventilation costs by a factor of up to six compared with oscillatory flow in a tube without the tail-fan constriction.

Key words: burrow ventilation, particle image velocimetry, PIV, tube-dwelling shrimp, *Callianassa subterranea*, metachrony, ventilation energetics, laminar flow, non-pulsating flow.

Introduction

Thalassinid shrimps characteristically create and inhabit burrows in the sea bed. These burrows are regularly ventilated for respiratory purposes or to filter the flow through the burrow for food (Atkinson and Taylor, 1988). The ventilation flow is generated by metachronal beating of three or four pairs of abdominal appendages, the pleopods (Farley and Case, 1968; Dworschak, 1981). Burrow ventilation is assumed to be energetically expensive and always occurs periodically (Atkinson and Taylor, 1988; Farley and Case, 1968; Torres *et al.* 1977; Felder, 1979; Dworschak, 1981; Mukai and Koike, 1984; Scott *et al.* 1988; Forster and Graf, 1995; Stamhuis *et al.* 1996). The predominantly filter-feeding Upogebiae are estimated to spend up to half their time on burrow ventilation for feeding purposes (Dworschak, 1981). The non-filter-feeding thalassinids, e.g. most of the Callianassidae, only ventilate their burrows occasionally, to renew the burrow water for respiration (Farley and Case, 1968; Stamhuis *et al.* 1996). Ventilation is performed in longer bouts with shorter intervals in the Upogebiae compared with the Callianassidae (Dworschak, 1981; Mukai and Koike, 1984; Forster and Graf, 1995; Stamhuis *et al.* 1996). Filter-feeding thalassinids, e.g. *Upogebia pusilla* and *Upogebia major*, use pumping rates of 33–50 ml min^{-1} (Dworschak, 1981; Koike and Mukai, 1983). In these species, ventilation mainly serves feeding purposes and is occasionally performed for respiration only (Scott *et al.* 1988).

The Callianassidae usually inhabit extended burrows and have other feeding strategies (Griffis and Suchanek, 1991). Water is pumped through the burrow mainly for respiration. Occasionally, sediment is expelled from the burrow by pumping, causing a plume at the sediment surface (e.g. Suchanek, 1983; de Vaugelas, 1985; Stamhuis *et al.* 1996). Ventilation pumping rates of 0.6–5.5 ml min^{-1} have been observed in *C. japonica* (Koike and Mukai, 1983; Mukai and Koike, 1984).

Flow through a burrow may be assisted directly by the

ambient flow or indirectly as a result of 'chimney effects' at elevated exhalant openings (Vogel, 1978, 1994). This may reduce the ventilation costs in some upogebian species (Allanson *et al.* 1992). Flow generation mechanisms in burrow-living animals have been studied mainly in tube-living worms (e.g. MacGinitie, 1939; Chapman, 1968; Brown, 1975, 1977; Riisgaard and Larsen, 1995). Flow generation by metachronally beating pleopods (or other appendages) is observed in thalassinids, but the resultant flow inside the burrow has not previously been studied quantitatively.

The thallassinid shrimp *Callianassa subterranea* creates and inhabits an extensive burrow in the seabed (Witbaard and Duineveld, 1989; Atkinson and Nash, 1990; Rowden and Jones, 1995; Stamhuis *et al.* 1997). The shrimp ventilates its burrow every 14 min for 1.3 min, which is approximately 8 % of its time budget (Stamhuis *et al.* 1996). This may account for a significant part of its energy budget. The ventilation flow is produced by active pumping with three pairs of pleopods in an ad-locomotory metachronal pattern at a frequency of approximately 1 Hz (Stamhuis and Videler, 1997*a*). The present paper describes quantitatively the ventilation flow in the burrow and in the vicinity of a pleopod-pumping *C. subterranea*. Flow fields in front of, around and behind the shrimp are analyzed and processed to velocity profiles. The flow is examined for pulsation, and the energetic advantages of different ventilation strategies are evaluated.

Materials and methods

Collection of animals

Callianassa subterranea (Montagu) of approximately 40 mm total length were collected from box core sediment samples at the Oyster Grounds, central North Sea, approximately 53°45′N and 4°30′E. A sampling trip was made in September 1992 on the Dutch research vessel '*Pelagia*'. Each specimen was stored and transported to the laboratory in a separate jar. In the laboratory, each animal was allowed to construct a burrow in a 5 or 10 l plastic container largely filled with sediment from the sampling site and stored submerged in seawater aquaria at 12 °C. For details of the collection procedures, transport, storage and handling conditions, see Stamhuis *et al.* (1996).

Experimental arrangement for recording the flow

To record the ventilation current of *C. subterranea*, individual animals were placed in a simple artificial burrow, a U-shaped glass tube of 8 mm diameter with two turning chambers at the ends of the horizontal section (Fig. 1). The burrow was submerged in a glass aquarium (width 5 cm) containing artificial sea water. The temperature of the experimental aquarium was kept at 12 °C by mounting it against a flat water-cooled heat exchanger, using ordinary hair-styling gel as a contact agent. Neutrally buoyant polystyrene particles with a diameter of approximately 25 μm were added to the water in the aquarium. The particles were illuminated by a vertical laser light sheet, approximately 0.5 mm thick, using a red light Krypton laser (wavelength 647 nm, P_{max} 1 W). The laser sheet coincided with the central plane of the glass tube. Images of the illuminated particles were taken using a high-resolution video camera equipped with a macro lens, mounted normal to the light sheet. The camera was electronically shuttered to prevent motion blur. The video frames were recorded using a U-matic-SP video recorder with access to

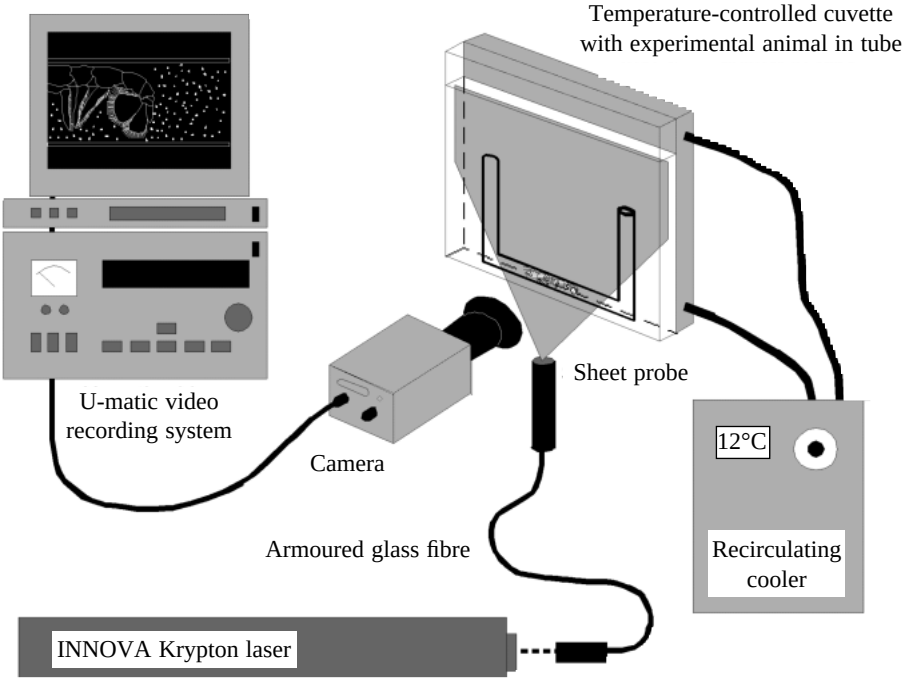

Fig. 1. Experimental arrangement showing the laser sheet illuminating the central vertical plane of a Perspex burrow in a cooled cuvette. Particle displacements in the illuminated plane, caused by *Callianassa subterranea* pumping, are recorded on video and later processed to vector flow fields.

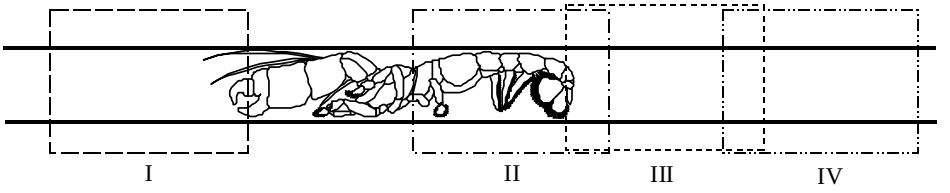

Fig. 2. A mudshrimp *Callianassa subterranea* (total length approximately 40 mm) in a tube in the active ventilation posture. The large rectangles labelled with Roman numerals indicate the tube sections in which the flow was analyzed.

each of the separate fields of a video frame (i.e. 25 frames s^{-1}, 50 fields s^{-1}).

The flow generated by a ventilating *C. subterranea* in the horizontal glass tube was recorded in four areas: in front of the animal, around the beating pleopods, directly behind the telson and further behind the animal (Fig. 2). The normal ventilation posture of *C. subterranea* allowed mainly lateral views but, since the shrimps sometimes turn around their longitudinal axis during ventilation, some views from the ventral and dorsal aspects were recorded as well. Ventilation flows generated by five different animals were recorded, and all showed the same flow patterns. The results from one animal are presented.

Image processing and flow analysis

To prevent video interlace blurring, single fields were used for analysis. The first fields of two successive video frames were digitized to 768×512 pixel images which were enhanced by background equalization and contrast stretching (TIM image-processing environment, DIFA Vision Systems). Displacements of particles were obtained at sub-pixel accuracy by applying a combination of particle-tracking velocimetry (PTV) and sub-image correlation particle image velocimetry (SCPIV) (Stamhuis and Videler, 1995). The flow patterns in front of and behind the experimental animals were analyzed using SCPIV, the flow around the beating pleopods had to be analyzed using PTV because of the large velocity gradients. Velocity vector maps derived from the particle displacement data were processed to complete flow fields by two-dimensional spline interpolation, after vector validation. The resulting vector flow fields consist of arrays of vectors describing the velocity magnitudes and directions of the local flow. Vector averaging in the direction of the longitudinal axis of the tube resulted in average local flow profiles. Gradient variables derived from the velocity flow fields were used to study and describe the flow morphology (Stamhuis and Videler, 1995). Pulsation of the flow was studied by tracking single particles in the main stream over time.

Results

The flow in the tube in front of a pumping *C. subterranea* is unidirectional (Fig. 3). The velocity profiles in the tube's median plane are almost perfectly parabolic throughout the tube, indicating fully developed laminar 'Hagen–Poiseuille' flow. No irregularities or backflows near the tube walls indicating major oscillations are found (Fig. 4).

Tracking of individual particles in the main stream in time shows the flow to be practically non-pulsatile (Fig. 5, region I). The maximum core velocity is approximately 4.0±0.2 mm s^{-1} (mean ± S.D., N=29), the mean velocity in the tube is therefore 2.0±0.1 mm s^{-1}.

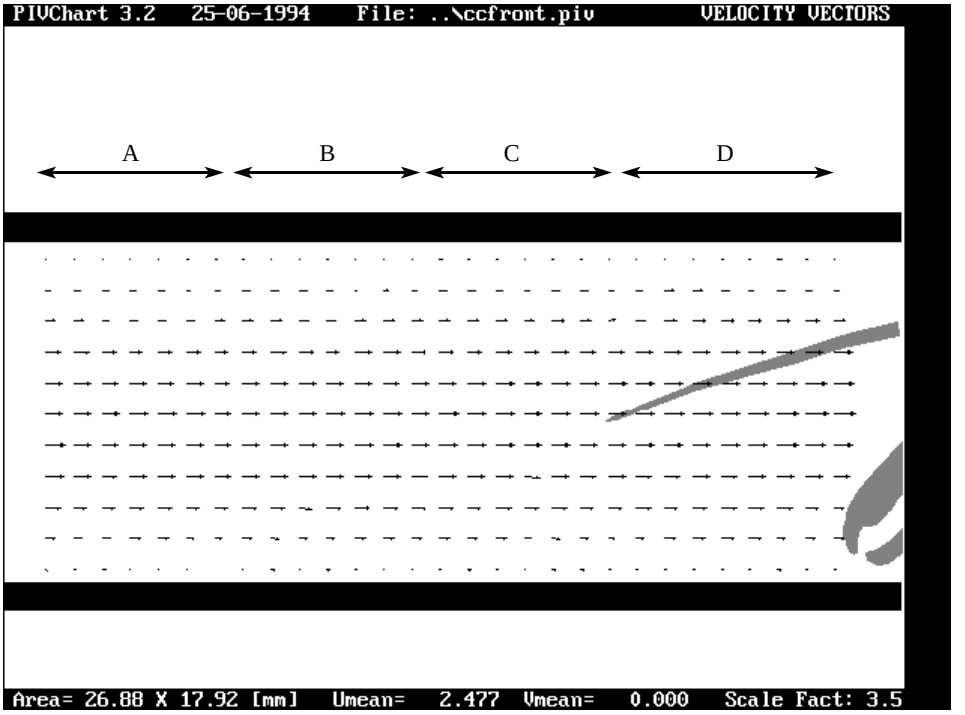

Fig. 3. Vector diagram of the flow in front of a pumping *Callianassa subterranea* in an artificial burrow (area I in Fig. 2). Inner tube diameter 10 mm; the animal is sitting on the right; a large cheliped and a large antenna are just visible. The labels A–D refer to Fig. 4.

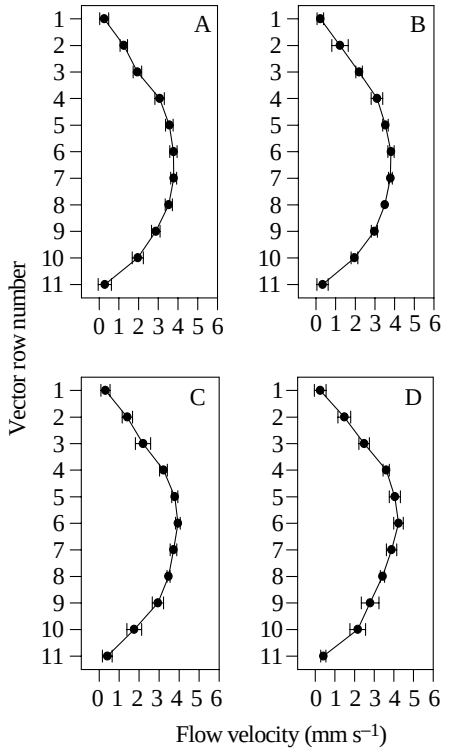

Fig. 4. Velocity profiles of four consecutive subsections of the flow in the tube in front of the shrimp, showing mean velocities (± S.D., *N*=7) for each row of vectors. The labels A–D refer to the areas indicated in Fig. 3.

Immediately in front of the abdomen, the flow is confined to the narrow space between the tube wall and the shrimp's thorax (Fig. 6, left part). The velocity near the tube wall is increased compared with the flow velocity in front of the animal (Fig. 4) because of the reduced cross-sectional area (Fig. 7A). Ventral to the abdomen, the flow is dominated by the oscillating pleopods (Fig. 6, middle part). During the power stroke, each pleopod acts like an oar accelerating a mass of adhering water during the first part of the power stroke. In the lower part of the tube (see Fig. 6), the water is mainly accelerated by the distal part of the pleopods and the extended pleopodal rims, which enter this region during the power stroke only. The water mass around the pleopod is shed in a ventro-caudal direction during the second half of the power stroke (Fig. 8A first pleopod, Fig. 8B second pleopod). Shedding of the water mass is facilitated when water is squeezed from the spaces between neighbouring pleopods as they approach one another (due to metachrony), mainly during the second half of the power stroke (Fig. 8B, between the second and third pleopods). Acceleration and shedding of bodies of water results in significant velocity gradients in the area of the beating pleopods (Fig. 5, region II). The net result of the pleopod action is an average water displacement converging towards the lower tube wall with an increasing flow velocity in a caudal direction (Fig. 7B–D). The water leaves the area of the pumping pleopods only through the narrow opening underneath the telson because the uropods close off the rest of the tube diameter. The water is ejected as a jet with a mean velocity approximately eight times the velocity of the undisturbed flow in front of the shrimp (Fig. 6, right part; Fig. 7D,E).

The velocity field directly behind the animal shows the high-velocity jet below a separation zone directly behind the telson (Figs 9, 10). In the separation zone, vortex-like backflow occurs with low velocity compared with that of the jet core. The jet coming from the opening underneath the telson continues to converge for a short distance downstream of the telson, the narrowest part (the 'vena contracta') being situated approximately 0.15 tube diameters behind the opening (Fig. 6, right side). From there, the jet diverges and the core velocity decreases because of the steep velocity gradient surrounding the jet core. The transverse velocity gradients are caused by shear between the jet core and the tube wall below the jet as well as between the jet and the slowly rotating separation zone above it (Fig. 9, colour coding). Because of the high rates of shear, the jet evolves towards a parabolic velocity profile within a distance of approximately 2.5 tube diameters behind the animal, which is less than one body length (see also Fig. 5, region III).

In Fig. 11, the animal had turned around its longitudinal axis, allowing a dorsal view of the abdominal region. This figure shows the blocking of the tube by the tail-fan, since the last abdominal segments, the uropods and the telson close off the tube almost completely, preventing leakage along the top and the sides. The flow passes only through the small opening ventral to the telson and emerges (in Fig. 11) some distance behind the telson, when it enters the central plane of the tube. The separation zone with low-velocity backflow is visible directly behind the telson in this figure.

Further downstream of the animal, the jet has faded and only small traces remain. (Fig. 12; area IV in Fig. 2). The flow

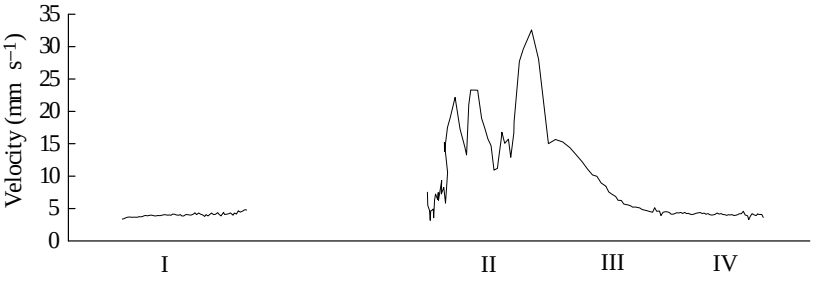

Fig. 5. The flow velocity as a function of position in the tube, with respect to the pumping *Callianassa subterranea*. Roman numerals I–IV indicate the areas of interest indicated in Fig. 2.

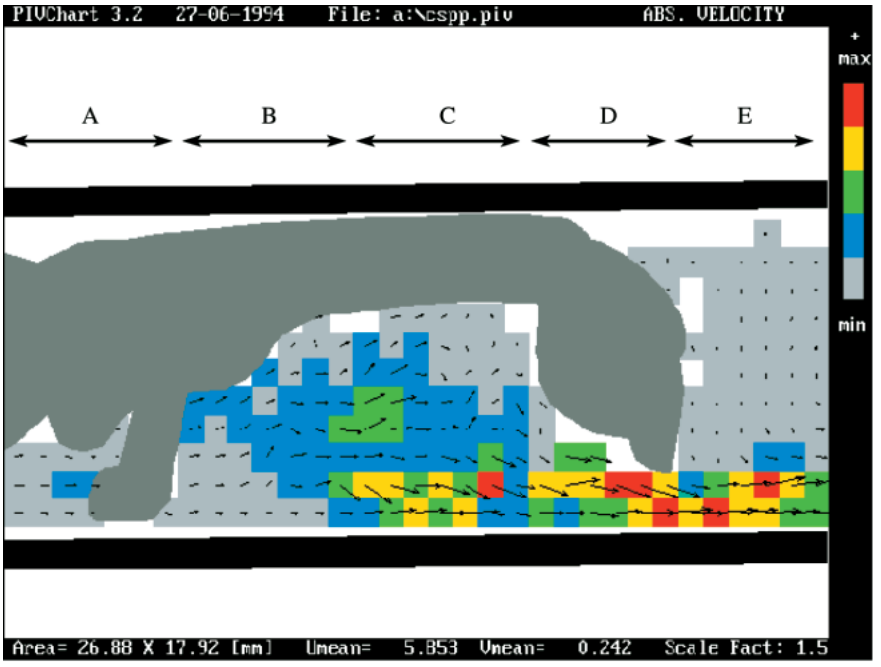

Fig. 6. Vector diagram of the flow around the pumping pleopods of *Callianassa subterranea* (area II in Fig. 2), averaged over a whole pumping cycle (22 steps of 0.04 s). The velocity is colour-coded to emphasize the flow morphology. The flow is vortical in the area where the pleopods are active (the pleopods are omitted for clarity). High flow velocities are observed in the lower part of the tube, where the pleopod tips accelerate the water during their power stroke. Labels A–E refer to Fig. 7.

profile in the tube gradually returns to the parabolic velocity profile normal for laminar flow (Fig. 13).

The flows in front of, around and behind a pumping *C. subterranea* are summarized in Fig. 14. This figure also shows reconstructed cross sections of characteristic positions in the tube to clarify further the morphology of the flow.

Discussion

In this discussion, our results will be compared with theoretical and empirical predictions. The energetic implications of different flow regimes will be quantified and evaluated. Finally, our results will be compared with data in the literature on thalassinid ventilation flows.

The flow in the burrow in the vicinity of a pumping *C. subterranea* matches predictions for non-pulsating laminar flow in a tube at low Reynolds number ($Re \approx 20$). The flow in front of the shrimp shows a parabolic velocity profile, which is characteristic of Hagen–Poiseuille flow (Prandtl and Tietjens, 1957). This is also the case for the flow profile downstream of the animal. A sudden expansion directly behind a constriction, as behind the telson of *C. subterranea*, usually causes a local separation zone with backflow near the tube wall (Caro *et al.* 1978; Munson *et al.* 1994). The parabolic velocity

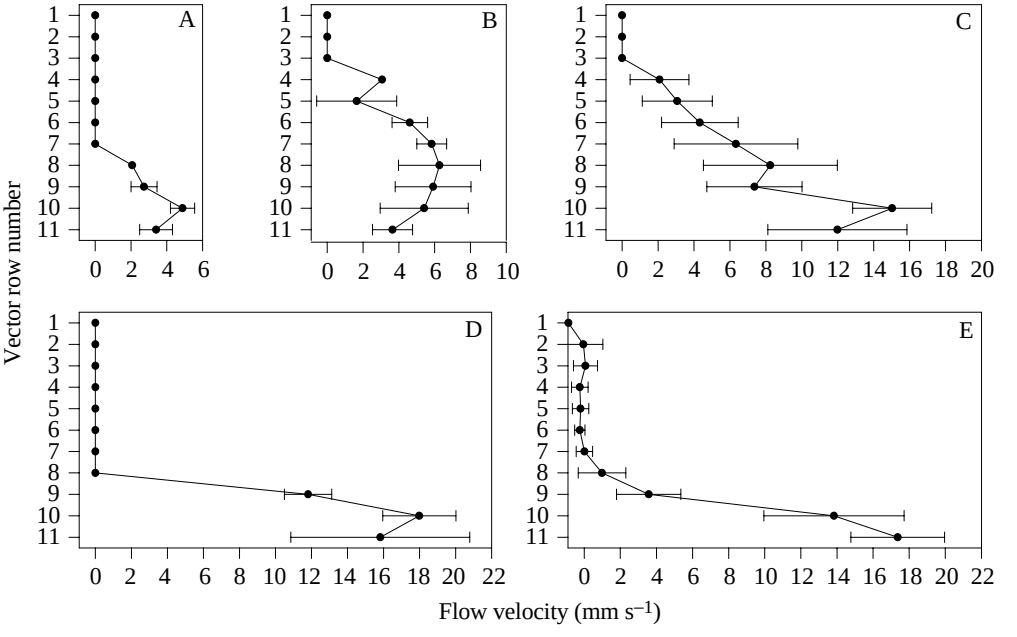

Fig. 7. Velocity profiles of five consecutive subsections of the tube in area II (see Fig. 2), showing the flow velocities around the abdomen (means ± S.D., N=7) for each row of vectors, averaged over a whole pumping cycle. A–E refer to the areas indicated in Fig. 6.

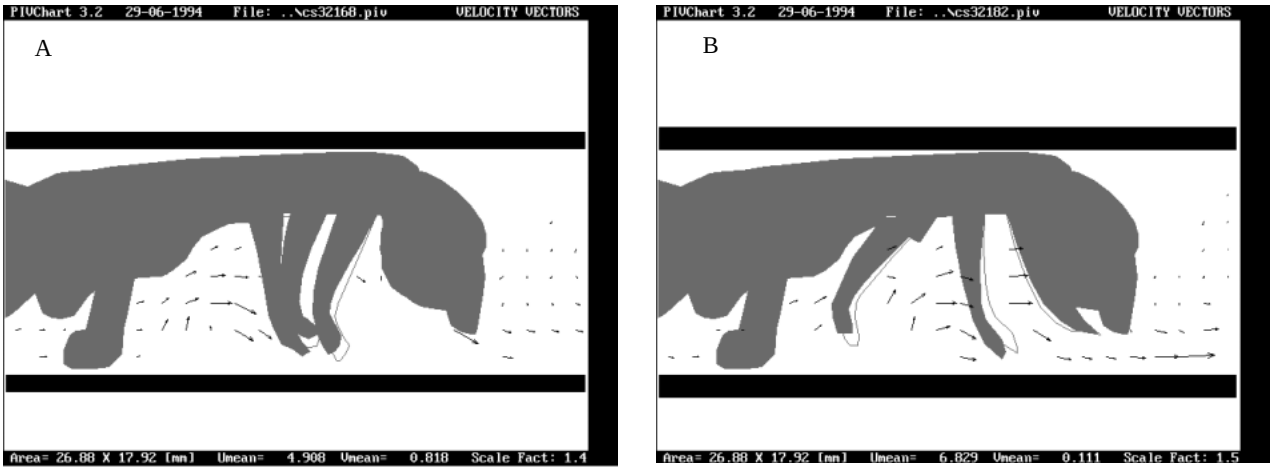

Fig. 8. Vector diagrams of the flow around the pumping pleopods during two stages of the pumping cycle with a phase difference of 0.64 cycle (14 steps of 0.04 s), showing the formation and degradation of rotational flow patterns between the pleopods due to the acceleration and shedding of water mantles. (A) The first pleopod has almost finished a power stroke, the second pleopod is making a recovery stroke, the third pleopod has just started a power stroke; (B) the first pleopod is starting a power stroke, the second pleopod is half-way through a power stroke, the third pleopod has just started a recovery stroke.

profile is restored within a short distance behind the telson. This is normal for laminar flow at low *Re*, showing limited transition effects at tube entrances, constrictions and expansions (Prandtl and Tietjens, 1957). The effects of pulsation of the flow can be evaluated and predicted by the Womersley number *Wo* (Caro *et al.* 1978). This dimensionless parameter is a function of the tube diameter *D*, the angular frequency ω and the kinematic viscosity ν:

$$Wo = \frac{D}{2}\sqrt{\frac{\omega}{\nu}}\,. \qquad (1)$$

When $Wo<1$, the flow resembles a normal Poiseuille flow. For $1<Wo<3$, the phase of the flow rate Q starts to lag behind the phase of the pressure gradient Δp_0, and the parabolic velocity profile becomes disturbed by the oscillatory motion of the fluid core. If $Wo>3$, Q lags more than 60° behind Δp_0, and inertial forces rule the flow, causing the velocity profile to flatten (Caro *et al.* 1978). The hydrodynamic resistance of a tube increases with *Wo*, causing a decrease in Q at values of $Wo \gg 1$.

In our experiments, $Wo \geqslant 12.5$ with $D=0.01$ m and $\omega=2\pi$ (pulsation frequency, $f=1$ Hz), predicting a strong pulsatory flow, an almost flat velocity profile, a phase shift between Q and Δp_0 of almost 90°, and a strongly reduced flow rate of approximately $0.1Q_{steady}$, where Q_{steady} is the non-pulsating

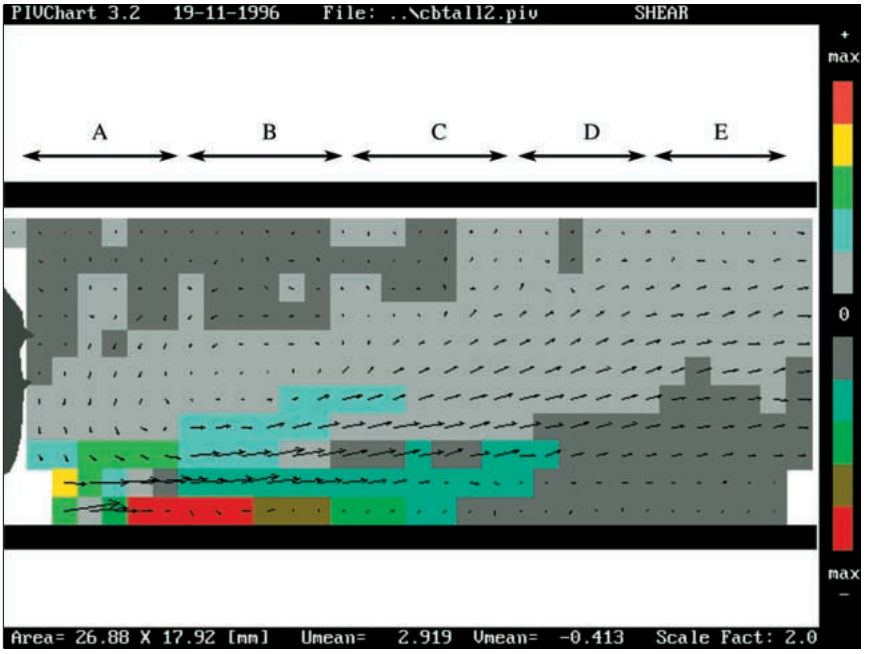

Fig. 9. Diagram showing the velocity vectors of the flow directly behind a pleopod-pumping *Callianassa subterranea* (area III in Fig. 2). The jet with high core velocities coming from underneath the telson (just visible on the left) diverges over the tube diameter with increasing distance behind the shrimp. Directly behind the telson, a large slowly rotating vortex system is formed due to separation. The colour coding shows the relative rate of shear. The relative maxima indicate the steep transverse velocity gradients at the tube wall and in the area between the jet and the slowly rotating area of water behind the telson. Labels A–E refer to Fig. 10.

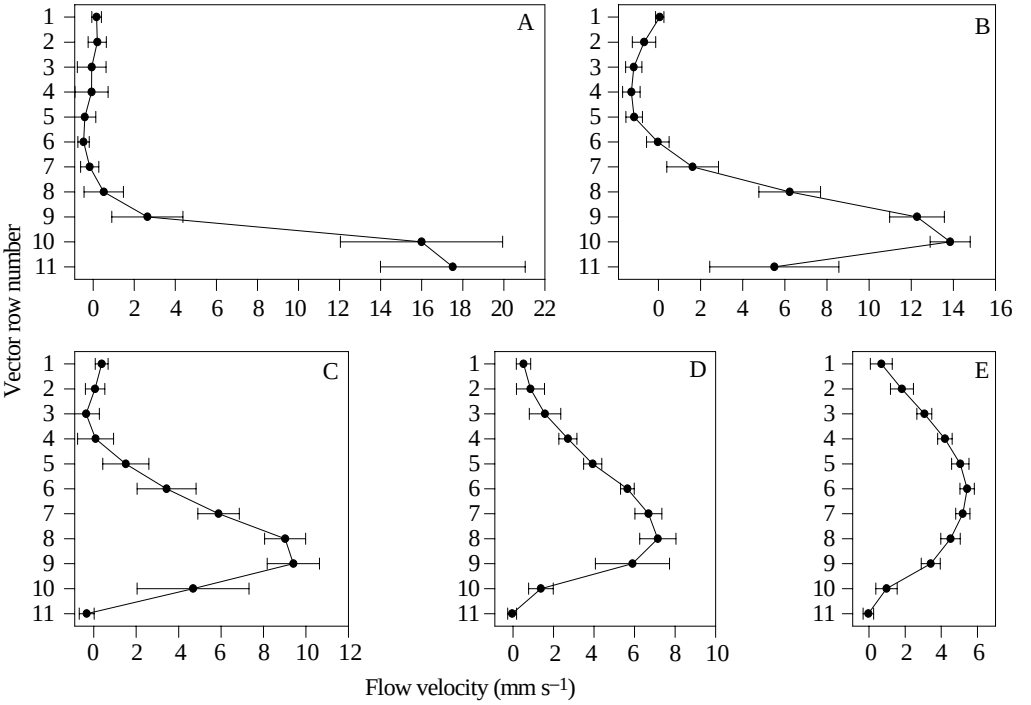

Fig. 10. Velocity profiles of five consecutive subsections of area III of the tube (see Fig. 2) showing the backflow directly behind the telson and the jet which evolves progressively towards a parabolic velocity profile (means ± S.D., *N*=7). Labels A–E refer to corresponding areas in Fig. 9.

laminar flow rate. However, the flow actually generated by *C. subterranea* resembles laminar flow with no trace of pulsation and no disturbance of the normal velocity distributions.

The fact that the flow in the tube is not pulsating can be explained from the geometry and kinematics of the 'pump'. The uropods and telson constrict the tube diameter. This reduces the cross-sectional area by a factor of approximately 10, thereby increasing the local mean flow velocity by the same factor. Some distance before the constriction, the flow converges towards the small opening. Directly behind the constriction, the jet flow converges further until the 'vena contracta' and then diverges. The flow velocity in the jet decreases only gradually, because of separation and the consequential rotating water mass behind the telson. As a result, the high flow velocity persists over a trajectory much longer than the constriction itself. This high flow velocity causes inertial forces to prevail over viscous forces, the local *Re* increases to values near 150 and the local *Wo* decreases to values close to 1. The character of the flow therefore changes locally from viscosity-dominated to inertia-dominated, which suppresses the expression of pulsation.

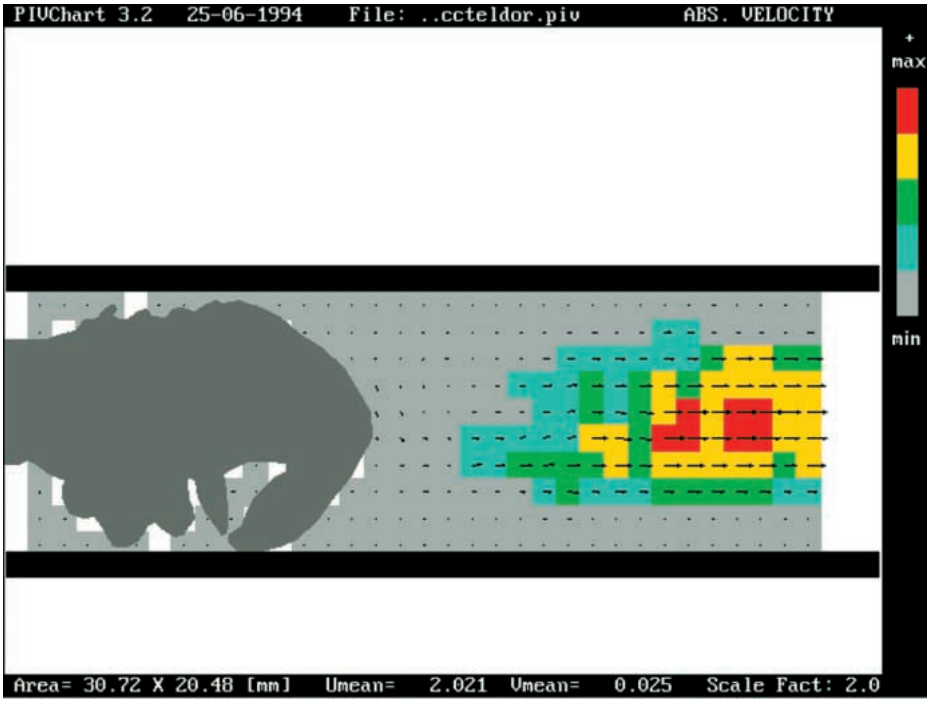

Fig. 11. Velocity magnitude (colour-coded) projected on the vector diagram of the flow directly behind the abdomen of a pumping *Callianassa subterranea* viewed from the dorsal aspect. No water passes the uropods, illustrating the way in which the tube is closed off. Behind the telson, small vectors indicating the downward component of the large vortex are visible. The diverging jet from underneath the telson comes into the plane of view on the right, showing high core velocities.

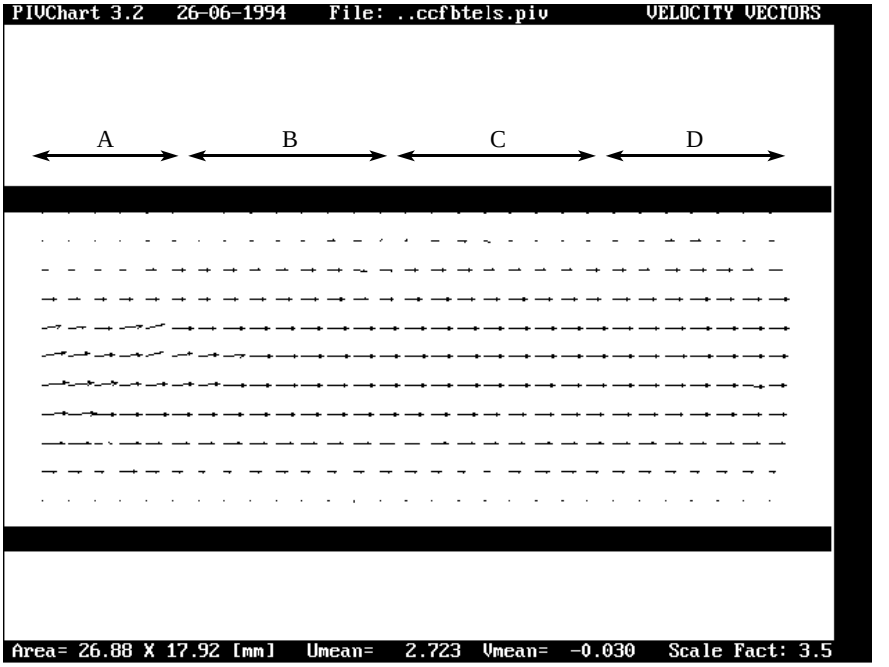

Fig. 12. Vector diagram of the flow further downstream of a pleopod-pumping *Callianassa subterranea* (area IV in Fig. 2). The jet has almost completely faded and the flow shows only minor remnants. Labels A–D refer to Fig. 13.

Furthermore, the pleopod movements during the recovery stroke are not the opposite of those during the power stroke. During the power stroke, the pleopods are fully extended into the main stream. During the recovery stroke, they are 'lifted' out of the main stream and reduce the flow velocity relatively little. The pleopods therefore act like oars, and the flow in the area of the oscillating pleopods is mainly confined to the lower part of the tube (see also Stamhuis and Videler, 1997*a*). Consequently, hardly any pulsation is generated.

The pleopods move in an ad-locomotory metachronal wave with a phase shift of approximately one-third of a cycle. This phase shift increases the pulsation frequency by a factor of three, but reduces the amplitude of a pulsation by approximately the same factor. Theoretically, the frequency increase would double *Wo* but, since the amplitude is practically zero, the flow is hardly affected.

Finally, the pleopod pump system of *C. subterranea* has a slip component, unlike a piston pump with valves. A piston pump imposes pulsation on the fluid because the fluid has to follow the piston displacement. Moving pleopods do not close off the tube completely, so that water can still flow around the tips. This damps pressure differences and promotes steady flow.

In conclusion, *C. subterranea* applies a combination of mechanisms to minimize pulsation in the flow through its burrow. It constricts the tube with its tail-fan, thereby locally changing the morphology and character of the flow, and it employs a pump with metachronally moving oar-like pleopods.

Fig. 15 is a diagram of the streamlines of a modelled laminar non-pulsatile flow in a tube of comparable geometry to that in the present study with a *C. subterranea* present, but without oscillating pleopods. This prediction was generated by solving the Navier–Stokes equations numerically in two dimensions, at the flow rate and Reynolds number that apply to the burrow of *C. subterranea* (Forbes and Recktenwald, 1996). The diagram matches our observations of the flow in the vicinity of the shrimp, confirming the laminar non-pulsatile character of this flow.

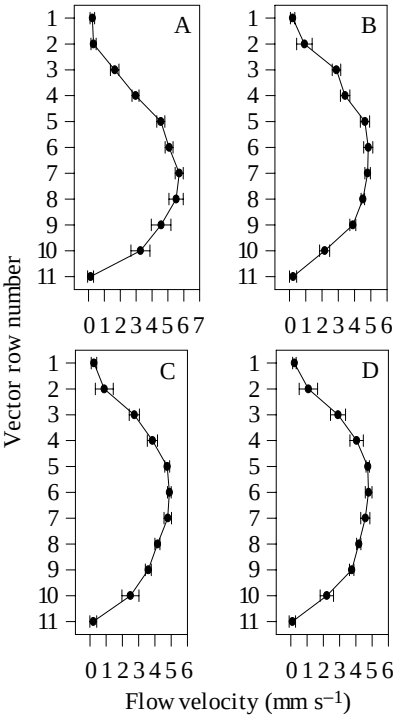

Fig. 13. Velocity profiles of four consecutive subsections of the tube in area IV (see Fig. 2), showing restoration of a parabolic velocity profile (means ± S.D., *N*=7). Labels A–D refer to the corresponding areas in Fig. 12.

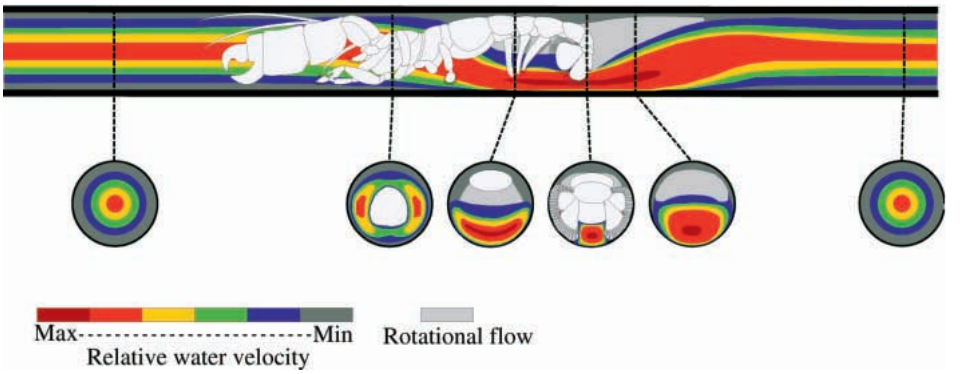

Fig. 14. Composite picture of the flow in a tube in front of, around and behind a pleopod-pumping *Callianassa subterranea* based on the results presented in this study. The colour coding gives an impression of the mean magnitude and direction of the flow. The cross sections of areas where significant changes take place, reconstructed from the results, illustrate the flow morphology.

Calculations of the dissipated mechanical energy for a tube with or without a constriction and with or without a pulsatory component in the flow yield estimates of the mechanical energy involved in *C. subterranea* ventilation at different flow regimes. The power necessary to maintain a steady laminar flow in a tube containing a pumping *C. subterranea* may be calculated by assuming that the animal in its tube resembles a straight cylindrical tube of length L_{tot} and diameter D_1 with two constrictions (Fig. 16).

The first constriction is a reduction of the tube diameter to $0.85D_1$ over a distance of 5 cm, representing a reduction in cross-sectional area to approximately 70 % due to the shrimp's body. The second constriction, immediately behind the first, reduces the tube diameter to $0.32D_1$, representing a reduction in cross-sectional area by the uropods and the telson by a factor of 10.

The total pressure difference to maintain flow in the tube is the sum of the partial pressure differences to (A) accelerate water into the tube entrance, (B) adjust a parabolic velocity profile, (C) overcome the viscous drag of the tube section upstream of the animal, (D) accelerate the flow into the first constriction, (E) overcome the viscous drag of the first constricted section, (F) accelerate the flow into the second constriction, (G) compensate for the pressure drop caused by separation, and (H) overcome the viscous drag of the tube section downstream of the animal. For reasons of clarity, these can be grouped according to the three distinct tube sections: (1) the upstream tube section (A+B+C); (2) the constrictions (D+E+F); and (3) the downstream tube section (G+H). The pressure drops for these sections can be calculated from the following equations (Prandt and Tietjens, 1957; Schlichting, 1979; Munson *et al.* 1994):

$$\Delta p_1 = \frac{\rho \overline{U_1}^2}{2} + \frac{1.2\rho \overline{U_1}^2}{2} + \frac{8\mu L_1 \overline{U_1}}{(0.5D_1)^2}\,, \tag{2}$$

$$\Delta p_2 = \frac{\rho(\overline{U_2} - \overline{U_1})^2}{2} + \frac{8\mu L_2 \overline{U_2}}{(0.5D_2)^2} + \frac{\rho(\overline{U_c} - \overline{U_2})^2}{2}\,, \tag{3}$$

$$\Delta p_3 = \frac{\rho(\overline{U_c} - \overline{U_3})^2}{2}\left(1 - \frac{A_c}{A_3}\right)^2 + \frac{8\mu L_3 \overline{U_3}}{(0.5D_3)^2}\,, \tag{4}$$

where ρ is the density, μ is the dynamic viscosity of sea water, $\overline{U}$ is the mean flow velocity, A is the cross-sectional area of the tube section and the subscripts 1, 2, 3 and c refer to the respective tube sections and the narrow constriction. The dissipated power P_0 is the product of the flow rate Q_0 and the pressure gradient Δp_{tot}:

$$P_0 = Q_0 \Delta p_{tot}\,, \tag{5}$$

where

$$\Delta p_{tot} = \Delta p_1 + \Delta p_2 + \Delta p_3 \tag{6}$$

and

$$Q_0 = \overline{U_1}\pi(0.5D_1)^2\,. \tag{7}$$

The tube dimensions and the mean velocity in tube section 1 are chosen to equal the experimental situation: D_1=0.01 m, L_1=L_3=0.20 m, L_2=0.05 m, L_c=0 and $\overline{U}$=0.002 m s^{-1}. The power dissipated by the water during normal ventilation flow in *C. subterranea*, assuming steady laminar flow throughout the tube, is found to be P_0=0.115×10^{-6} W.

A similar approach can be followed to calculate the dissipated power for a pulsatile flow with the same mean flow rate. Since minimization of pulsation in *C. subterranea* is

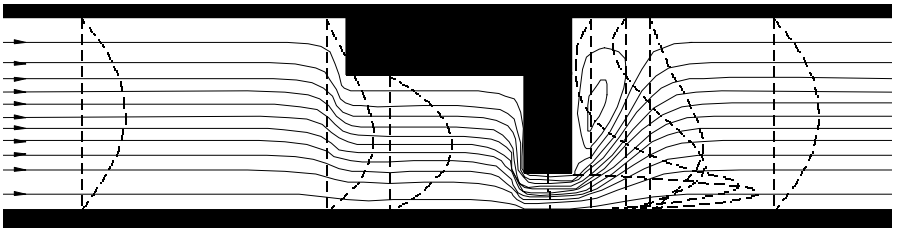

Fig. 15. Simulation of the flow in a tube in the vicinity of a pumping *Callianassa subterranea*, obtained by solving the Navier–Stokes equations numerically for a 60×40 grid, projected onto a 20 cm long and 1 cm wide tube. The streamlines are shown as thin lines, the cross-sectional velocity profiles as broken lines, and the shrimp is depicted as two consecutive constrictions (see text). The tube is displayed with a smaller aspect ratio to give a clearer picture. The simulation was performed using QnS, a two-dimensional computer fluid dynamics program for laminar flow.

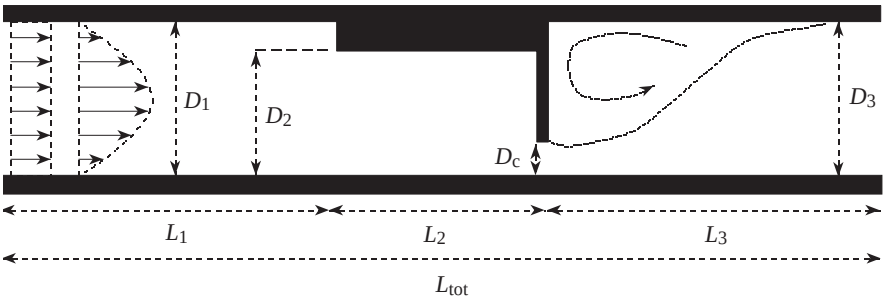

Fig. 16. Model of *Callianassa subterranea* in a tube, to show the hydrodynamic events, cross-sectional velocity profiles and dimensional variables used in the equations for calculating the pressure drop and the dissipated energy. *D*, diameter; *L*, length; subscripts 1, 2, 3 and c refer to the respective tube sections and the narrow constriction; L_{tot}, total tube length.

concluded to be due to the tube constriction, the dissipated power is calculated for a pulsating flow passing through a straight cylindrical tube without constrictions and of the same total length. The minor constriction due to the animal's body is neglected to enable an analytical solution of the problem. Assuming a sinusoidal oscillatory flow component superimposed on a steady flow, the mean velocity $\overline{U}_t$ of the flow in the tube can be expressed as:

$$\overline{U}_t = \overline{U}_1 + \overline{U_{osc}}\sin\omega t\,, \tag{8}$$

where $\overline{U_{osc}}$ is the maximum mean oscillatory velocity and t is time. The mean flow velocity equals the situation without oscillatory flow. The pressure gradient inducing pulsating flow is assumed to consist of a steady part and a superimposed unsteady part. It consists of components for accelerating water into the tube entrance, adjusting a parabolic velocity profile, overcoming the viscous drag of the whole tube and compensating for the unsteady pressure drop. These pressure drops can be calculated from equations 9 and 10 (Prandtl and Tietjens, 1957; Schlichting, 1979; this study):

$$\Delta p_{steady} = \frac{\rho\overline{U}_1^2}{2} + \frac{1.2\rho\overline{U}_1^2}{2} + \frac{8\mu L_{tot}\overline{U}_1}{(0.5D_1)^2}\,, \tag{9}$$

$$\Delta p_{unsteady} = \rho L_{tot}\frac{dU_t}{dt} = \rho L_{tot}\omega\overline{U_{osc}}\cos(\omega t)\,. \tag{10}$$

The dissipated power for the steady flow component is:

$$P_{steady} = Q_0\Delta p_{steady}\,. \tag{11}$$

The dissipated power for the unsteady component is found after integrating $\Delta p_{unsteady}$ over one cycle and multiplying by Q_0:

$$P_{unsteady} = Q_0\rho L_{tot}\omega\overline{U_{osc}}4\int_0^{T/4}\cos(\omega t)dt = \pi D_1^2\rho L_{tot}\overline{U_{osc}}^2\,, \tag{12}$$

where T is the period time.

When calculating the steady and the unsteady dissipated power with L_{tot}=0.45 m, D_1=0.01 m, f=1 Hz and $\overline{U}_1=\overline{U_{osc}}$=0.002 m s^{-1}, the total dissipated power with unsteady flow $p_{tot,unsteady}$ can be calculated: P_{steady}=0.061×10^{-6} W, $P_{unsteady}$=0.579×10^{-6} W and $P_{tot,unsteady}=P_{steady}+P_{unsteady}$= 0.640×10^{-6} W.

Hence, by constricting the tube with its tail-fan, *C. subterranea* theoretically doubles the dissipated power ($P_0\approx 2P_{steady}$), but requires only one-sixth of the power that would be needed to produce oscillatory flow in a tube without the tail-fan constriction ($P_{tot,unsteady}\approx 6P_0$). Keeping the flow steady and laminar by partially constricting the tube and confining the flow ventral to the metachronally beating pleopods is therefore probably an energetically advantageous ventilation strategy.

It should be noted that the dissipated power is not necessarily equal to the mechanical power invested by the pumping shrimp, which is usually higher because of the pump efficiency and the muscle efficiency, which are less than 1 (Stamhuis and Videler, 1997*a*).

For a few thalassinid species, mainly Upogebiae, pumping flow rates are reported in combination with some information on an animal's posture and pleopod beating pattern (Dworschak, 1981; Allanson *et al.* 1992; Scott *et al.* 1988; Forster and Graf, 1995; Stamhuis and Videler, 1997*a*). The main differences between Upogebiae and Callianassidae regarding ventilation are the number of pleopods active in pumping, the morphology of the tail-fan, the mechanism of flow regulation and the average time spent pumping. Upogebiae, at least the filter-feeding species, spend much more time pumping (up to 45 %) than the Callianassidae as a result of their need to generate a flow for feeding purposes (Dworschak, 1981; Scott *et al.* 1988). In the Upogebiae, the uropods are approximately the same size as the telson with equally long setae, whereas in the Callianassidae the telson is smaller than the uropods and has very short setae (Stamhuis and Videler, 1997*a*). The ventilation flow in *Upogebia operculata* and *Upogebia* sp. is adjusted by changing the posture of the whole tail-fan (Scott *et al.* 1988), which is probably the case in most Upogebiae. *C. subterranea* does not change the posture of the tail-fan during pumping and, since the other Callianassidae have a similar tail-fan morphology, this is probably also the case in the other Callianassidae. The Upogebiae have four pairs of paddle-like pleopods, which are all used in pumping, but no records exist, to our knowledge, on motion patterns or phase shifts between pleopod pairs. As in *C. subterranea*, the Callianassidae have only three pairs of pleopods involved in pumping, with a phase shift of approximately one-third of a cycle (Stamhuis and Videler, 1997*a*). The flow rates during pumping in *Upogebia pusilla* are 2–4 times as high as in *C. subterranea* and *C. japonica* of the same size, at approximately the same or an even lower pleopod

beat frequency (Dworschak, 1981; Stamhuis and Videler, 1997*a*; Forster and Graf, 1995; Mukai and Koike, 1984).

These data on ventilation in thalassinid species indicate that the mechanism of minimizing pulsation in the ventilation flow in thalassinids may be applied in various ways. Our hydrodynamic predictions support this view. If the pleopod beat frequency and, consequently, the flow velocity is increased, it may be energetically advantageous to widen the constriction, since the hydrodynamic resistance of the constriction increases with the square of the velocity (third term in equation 3) and the dissipated power increases with the cube of the velocity. The other advantages of a high flow velocity are not necessarily affected by this strategy, since the increased flow velocity with a less narrow constriction will make inertial forces prevail over viscous forces. This, in combination with the increase in pump frequency, probably suppresses the expression of pulsation. Such a ventilation strategy is observed in *Upogebia operculata* and *Upogebia* sp. (Scott *et al.* 1988), and was also observed in *C. subterranea* during occasional heavy pumping to flush sediment out of the burrow. *C. subterranea* increased the pleopod beat frequency by a factor of approximately three and partly lifted its tail-fan while flushing out excavated sediment (see also Stamhuis *et al.* 1996).

Forster and Graf (1995) recorded ventilation activity of adult *C. subterranea* in mesocosms and found a rather different ventilation pattern from the one described in the present study. They measured the flow using a thermistor probe in inhalant or exhalant openings of burrows and found a pulsating flow with a pulsation frequency of 0.15 Hz, which they observed to correlate with the pleopod motions (1 beat cycle per 7 s). They found the mean flow rate to be 1.8±1.1 ml min^{-1} (mean ± S.D.). These results on pleopod beat frequency, flow rate and the pulsating character of the flow are all contrary to our results: we found a non-pulsating flow with a mean flow rate of 9.4±1.5 ml min^{-1} at a pleopod beat frequency of 0.9±0.2 Hz (see also Stamhuis and Videler, 1997*a*). We observed the ventilation behaviour of more than 20 animals during behavioural studies (Stamhuis *et al.* 1996) and recorded pleopod beat frequencies from five individuals during the experiments presented here. The beat frequency during ventilation appeared to be typically approximately 1 Hz in all animals. We rarely observed pleopod movement of very low frequency, which we did not classify as ventilation activity. Some animals did display these slow motion patterns on occasions, others never did. Owing to the very low beat frequency, the resulting low-velocity flow showed pulsatility, and obviously viscous forces dominated the flow. We suspect that Forster and Graf (1995) recorded this type of pleopod motion and the consequent flow pattern.

Our results on the dissipated power in the ventilation flow are of the same order of magnitude as estimated by Allanson *et al.* (1992) for *Upogebia africana* and by Gust and Harrison (1981) for the alpheid shrimp *Alpheus mackayi*, when accounting for differences in size and pumping rates. In those studies, however, the pressure drops at the entrance and at constrictions were not taken into account. Depending on the flow velocity and the dimensions of the constrictions, this may cause underestimations of the dissipated power by a factor two or more.

The present results on the velocity distributions and morphology of the flow in the vicinity of a pleopod-pumping *C. subterranea* will be used to model pleopod pumping energetics in tube-living thalassinids in companion paper (Stamhuis and Videler, 1997*b*).

We cordially thank Professor T. J. Pedley (University of Cambridge) for guidance on the fluid dynamics of tube flows, especially on entrance effects and oscillatory flow. We are indebted to Ulrike Müller for critically reading the first draft of the manuscript.

References

ALLANSON, B. R., SKINNER, D. AND IMBERGER, J. (1992). Flow in prawn burrows. *Est. Coast. Shelf Sci.* **35**, 253–266.

ATKINSON, R. J. A. AND NASH, R. D. M. (1990). Some preliminary observations on the burrows of *Callianassa subterranea* (Montagu) (Decapoda: Thallassinidea) from the west coast of Scotland. *J. nat. Hist.* **24**, 403–413.

ATKINSON, R. J. A. AND TAYLOR, A. C. (1988). Physiological ecology of burrowing decapods. In *Aspects of Decapod Crustacean Biology* (ed. A. A. Fincham and P. S. Rainbow). *Symp. zool. Soc. Lond.* **59**, 201–226. Oxford: Clarendon Press.

BROWN, S. C. (1975). Biomechenics of water-pumping by *Chaetopterus variopedatus* Renier. Skeletomusculature and kinematics. *Biol. Bull. mar. biol. Lab., Woods Hole* **149**, 136–150.

BROWN, S. C. (1977). Biomechenics of water-pumping by *Chaetopterus variopedatus* Renier. Kinetics and hydrodynamics. *Biol. Bull. mar. biol. Lab., Woods Hole* **153**, 121–132.

CARO, C. G., PEDLEY, T. J., SCHROTER, R. C. AND SEED, W. A. (1978). *The Mechanics of the Circulation*. Oxford: Oxford University Press.

CHAPMAN, G. (1968). The hydraulic system of *Urechis caupo* Fisher and McGinitie. *J. exp. Biol.* **49**, 657–667.

DE VAUGELAS, J. (1985). Sediment reworking by callianassid mudshrimps in tropical lagoons: a review with perspectives. *Proc. 5th Int. Coral Reef Congr. Tahiti* **6**, 617–622.

DWORSCHAK, P. C. (1981). The pumping rates of the burrowing shrimp *Upogebia pusilla* (Petagna) (Decapoda: Thalassinidea). *J. exp. mar. Biol. Ecol.* **52**, 25–35.

FARLEY, R. D. AND CASE, J. F. (1968). Perception of external oxygen by the burrowing shrimp, *Callianassa californiensis* Dana and *C. affinis* Dana. *Biol. Bull. mar. biol. Lab., Woods Hole* **134**, 361–365.

FELDER, D. L. (1979). Respiratory adaptations of the estuarine mud shrimp, *Callianassa jamaicense* (Schmitt, 1935) (Crustacea: Thalassinidea). *Biol. Bull. mar. biol. Lab., Woods Hole* **152**, 134–146.

FORBES, S. AND RECKTENWALD, G. (1995). QnS, a Computational Fluid Dynamics program for laminar, incompressible flow in 2D cartesian or axisymmetric coordinate systems (freeware). http://www.me.pdx.edu/~gerry/QnS

FORSTER, S. AND GRAF, G. (1995). Impact of irrigation on oxygen flux into the sediment: intermittent pumping by *Callianassa*

subterranea and 'piston-pumping' by *Lanice conchilega*. *Mar. Biol*. **123**, 335–346.

GRIFFIS, R. B. AND SUCHANEK, T. H. (1991). A model of burrow architecture and trophic modes in thallassinidean shrimps (Decapoda: Thallassinidea). *Mar. Ecol. Prog. Ser.* **79**, 171–183.

GUST, G. AND HARRISON, J. T. (1981). Biological pumps at the sediment–water interface: Mechanistic evaluation of the Alpheid shrimp *Alpheus mackayi* and its irrigation pattern. *Mar. Biol*. **64**, 71–78.

KOIKE, I. AND MUKAI, H. (1983). Oxygen and inorganic nitrogen conditions and their fluxes in the burrow of *Callianassa japonica* [de Haan] and *Upogebia major* [de Haan]. *Mar. Ecol. Progr. Ser.* **12**, 185–190.

MACGINITIE, G. E. (1939). The method of feeding of *Chaetopterus*. *Biol. Bull. mar. biol. Lab., Woods Hole* **77**, 115–118.

MUKAI, H. AND KOIKE, L. (1984). Pumping rates of the mud shrimp *Callianassa japonica*. *J. Oceanogr. Soc. Japan* **40**, 243–246.

MUNSON, B. R., YOUNG, D. F. AND OKIISHI, T. H. (1994). *Fundamentals of Fluid Mechanics*. Second edition. New York: John Wiley & Sons.

PRANDTL, L. AND TIETJENS, O. G. (1957). *Applied Hydro- and Aeromechanics*. New York: Dover Publications (replica of 1934 edition).

RIISGAARD, H. U. AND LARSEN, P. S. (1995). Filter-feeding in marine macro-invertebrates: pump characteristics, modelling and energy cost. *Biol. Rev*. **70**, 67–106.

ROWDEN, A. A. AND JONES, M. B. (1995). The burrow structure of the mud shrimp *Callianassa subterranea* (Decapoda: Thalassinidea) from the North Sea. *J. nat. Hist*. **29**, 1155–1165.

SCHLICHTING, H. (1979). *Boundary-Layer Theory*. Seventh edition. New York: McGraw-Hill.

SCOTT, P. J. B., REISWIG, H. M. AND MARCOTTE, B. M. (1988). Ecology, functional morphology, behaviour and feeding in coral- and sponge-boring species of *Upogebia* (Crustacea: Decapoda: Thalassinidea). *Can. J. Zool*. **68**, 483–495.

STAMHUIS, E. J., REEDE-DEKKER, T., ETTEN, Y., VAN WILJES, J. J. AND VIDELER, J. J. (1996). Behaviour and allocation of time of the burrowing shrimp *Callianassa subterranea* (Decapoda, Thalassinidea). *J. exp. mar. Biol. Ecol.* **204**, 225–239.

STAMHUIS, E. J., SCHREURS, C. E. AND VIDELER, J. J. (1997). Burrow architecture and turbative activity of the thalassinid shrimp *Callianassa subterranea* from the central North Sea. *Mar. Ecol. Progr. Ser.* **151**, 155–163.

STAMHUIS, E. J. AND VIDELER, J. J. (1995). Quantitative flow analysis around aquatic animals using laser sheet particle image velocimetry. *J. exp. Biol.* **198**, 283–294.

STAMHUIS, E. J. AND VIDELER, J. J. (1997*a*). Burrow ventilation in the tube-dwelling shrimp *Callianassa subterranea* (Decapoda: Thalassinidea). I. Morphology and motion of the pleopods, uropods and telson. *J. exp. Biol.* **201**, 2151–2158.

STAMHUIS, E. J. AND VIDELER, J. J. (1997*b*). Burrow ventilation in the tube-dwelling shrimp *Callianassa subterranea* (Decapoda: Thalassinidea). III. Hydrodynamic modelling and the energetics of pleopod pumping. *J. exp. Biol.* **201**, 2171–2181.

SUCHANEK, T. H. (1983). Control of seagrass communities and sediment distribution by *Callianassa* (Crustacea, Thalassinidea) bioturbation. *J. mar. Res.* **41**, 281–298.

TORRES, J. J., GLUCK, D. L. AND CHILDRESS, J. J. (1977). Activity and physiological significance of the pleopods in the respiration of *Callianassa californiensis* (Dana) (Crustacea: Thalassinidea). *Biol. Bull. mar. biol. Lab., Woods Hole* **152**, 134–146.

VOGEL, S. (1978). Organisms that capture currents. *Scient. Am.* **239**, 108–117.

VOGEL, S. (1994). *Life in Moving Fluids: the Physical Biology of Flow*. Second edition. Princeton, NJ: Princeton University Press.

WITBAARD, R. AND DUINEVELD, G. C. A. (1989). Some aspects of the biology and ecology of the burrowing shrimp *Callianassa subterranea* (Montagu) (Thallassinidea) from the Southern North Sea. *Sarsia* **74**, 209–219.